Supporting Information Appendix

Midlife gene expressions identify modulators of aging through dietary interventions

Bing Zhou[a,b,c,1], Liu Yang[d,1], Shoufeng Li[d], Jialiang Huang[a,b,c], Haiyang Chen[e], Lei Hou[a,b,c], Jinbo Wang[c,e], Christopher D. Green[a], Zhen Yan[f], Xun Huang[e], Matt Kaeberlein[g], Li Zhu[h], Huasheng Xiao[h], Yong Liu[d,2] and Jing-Dong J. Han[a,2]

[a]Chinese Academy of Sciences Key Laboratory for Computational Biology, Chinese Academy of Sciences—Max Planck Partner Institute for Computational Biology, Shanghai Institutes for Biological Sciences, Chinese Academy of Sciences, Shanghai 200031, China; [b]Center for Molecular Systems Biology, Institute of Genetics and Developmental Biology, Chinese Academy of Sciences, Beijing 100101, China; [c]Graduate University, Chinese Academy of Sciences, Beijing 100049, China; [d]Key Laboratory of Nutrition and Metabolism, Institute for Nutritional Sciences, Shanghai Institutes for Biological Sciences, Chinese Academy of Sciences, Shanghai 200031, China; [e]State Key Laboratory of Molecular Developmental Biology, Institute of Genetics and Developmental Biology, Chinese Academy of Sciences, Beijing 100101, China; [f]Departments of Medicine-Cardiovascular Medicine and Pharmacology and Center for Skeletal Muscle Research, Robert M. Berne Cardiovascular Research Center, University of Virginia, Charlottesville, VA 22908; [g]Department of Pathology, University of Washington, Seattle, WA 98195; and [h]Key Laboratory of Systems Biology, Shanghai Institutes for Biological Sciences, Chinese Academy of Sciences, Shanghai 200031, China

[1]B.Z. and L.Y. contributed equally to this work.

[2]To whom correspondence may be addressed. E-mail: liuy@sibs.ac.cn or jdhan@genetics.ac.cn.

Table of Contents

Supplemental Materials and Methods

Tightrope, rotarod and hair re-growth assays

For tightrope test, mice were placed on the middle of a bar of circular section (60 cm long; 3 cm in diameter). The test was considered successful when a mouse passed the tightrope during a period of 60 sec in at least one out of five consecutive trials. For rotarod test, each mouse was pre-trained at a constant speed (3 rpm) until it was able to remain on the apparatus for 60 sec. On the following day, each mouse was given three trials, with a 30-min rest period in between. During the test, the rotarod started at 3 rpm and accelerated to 24 rpm over a period of 9 min, the maximum length of each trial. For hair re-growth analysis, dorsal hair was removed by plucking from a square of approximately 1.5 cm×1.5 cm. Hair re-growth was scored three weeks later blindly by two other investigators from digital photographs and a semi-quantitative assessment was done using an arbitrary scale from one to four, where four represents complete hair regeneration.

Metabolic and serum measurements of mice

Total body fat content was measured by nuclear magnetic resonance (NMR) using the Minispec Mq7.5 (Bruker, Germany). Oxygen consumption and physical activity were measured using the comprehensive laboratory animal monitoring system (CLAMS, Columbus Instruments, Columbus, Ohio, USA) according to the manufacturers' instructions. Mice were allowed for acclimation to the CLAMS for 16-20 hours, and measurements were conducted for the following 24 hours. Voluntary activity was monitored from the x-axis beam breaks recorded every 15 min.

Glucose tolerance test was performed in mice after overnight fasting. Mice were injected

intraperitoneally with glucose at 1g/kg, and blood glucose concentrations were measured at 15, 30, 45, 60, and 120 min after insulin injection using a glucometer (FreeStyle, Alameda, CA).

Blood samples were collected from tail bleeding after overnight fasting in mice at the desired ages. After centrifugation at 12,000 rpm for 30 min to pellet blood cells, serum was transferred to a new tube and stored at -80 °C until further use. The serum levels of insulin and leptin were quantified by the Bioplex Suspension Array System (Bio-Rad) using a mouse cytokine immunoassay panel (Linco Research, St. Charles, MO). Serum triglyceride and cholesterol were respectively determined using the Serum Triglyceride Determination Kit (Sigma, St. Louis, MO) and Amplex Red Cholesterol Assay Kit (Molecular Probes, Eugene, OR).

Body temperature

The rectal body temperature was measured for mice at 90 weeks of age. The measurements were performed between 8:00 a.m. and 10:00 a.m. after an overnight fast using microprobe thermometer (Physitemp Instruments, Clifton, New Jersey, USA).

Liver physiological analysis

For midlife metabolic phenotype analyses, 8 mice at 62 weeks of age were randomly selected from each group and were humanely euthanized for blood and tissue collection. To analyze the liver function, serum levels of alanine transaminase (ALT) and aspartate transaminase (AST) were determined by the Alanine/Aspartate Transaminase Detection Kit (ShenSuoYouFu, Shanghai, China). To measure hepatic triglyceride and cholesterol levels, 40-50 mg of liver tissue were homogenized in 1.5 ml of $CHCl_3$-CH_3OH (2:1, v/v), followed by shaking at room temperature for 2 hr. After addition of 0.5 ml of 0.1 M NaCl, the suspension was centrifuged at 3,700 rpm for 10 min at room temperature. The lower organic phase was then transferred and air-dried overnight. The residual liquid was subsequently resuspended in 400 µl of 1% Triton X-100 in absolute ethanol, and the concentrations of triglyceride and cholesterol were determined using the Serum Triglyceride Determination Kit (Sigma, St. Louis, MO) and Amplex Red Cholesterol Assay Kit (Molecular Probes, Eugene, OR), respectively. For histology analysis, liver tissue specimens were fixed in 10% neutral formalin, and paraffin-embedded tissue sections were stained with hematoxylin-eosin (H&E) or picrosirius red (Sigma-Aldrich, St. Louis, MO). Three whole sections (4× magnifications) from each animal were examined by BX61 fluorescence microscope (Olympus, Japan) and images were quantified using NIH ImageJ software (http://rsb.info.nih.gov/ij/). For measurement of the mitochondria, liver tissues were processed as described (1). Briefly, livers that were cut into 1-mm^3 sections were subsequently put into the electron microscopy fixative buffer, embedded in spur resin and sectioned. Thin sections were obtained and viewed under transmission electron microscope (H-7650, HITACHI) equipped with a charge-coupled device camera (ER-B; AMT). Mitochondrial number was counted from images at 1200X and normalized to the hepatocyte size. The sizes of hepatocytes and mitochondria were quantified from images at 6000X by NIH ImageJ software.

Identification of aging patterns

Liver RNA samples from six mice at 4, 8, 13 or 21 months of age were respectively pooled and subjected to whole-genome microarray analyses following the same protocol as for the 18 mice from the intervention study. The microarray data were likewise log2-transformed and normalized using 'affy' package in bioconductor. The significance of age-related patterns was determined by STEM (2) ($P < 0.01$).

Visualization of the KEGG peroxisome pathway

KEGG peroxisome pathway was colored using the pathway visualization tool in KEGG (http://www.genome.jp/kegg/tool/color_pathway.html).

RT-PCR analyses

Total mouse liver RNA was isolated using TRIzol reagent (Invitrogen, Carlsbad, CA). After treatment with RNase-free DNase I (Roche Applied Science, Penzberg, Germany) to eliminate possible DNA contamination, first-strand cDNA was synthesized with M-MLV reverse transcriptase and random hexamer primers (Invitrogen). Real-time quantitative PCR was conducted with the SYBR Green PCR system (Applied Biosystems, Foster City, CA), using cyclophilin as an internal control for normalization. The oligonucleotide primers used for each target gene were as follows:
mouse *Pex1*, forward primer 5'-AGCTTGGTGGCACTCATCG-3' and reverse primer 5'-GTTCCGGATTGGGAGGCT-3';
mouse *Pex5*, forward primer 5'-AATGCAACTCTTGTATCCCGAG-3' and reverse primer 5'-GGCGAAAGTTTGACTGTTCAATC-3';
mouse *Pex13*, forward primer 5'-GATTTTGTTGCCGTGTCTGATG-3' and reverse primer 5'-TTTGACCGTCAAGACTAGCCAG-3';
mouse *Pxmp4*, forward primer 5'-TGTCTATGGAGTCAAAATCCGGG-3' and reverse primer 5'-AGAGTGGATGTACGTGGCTTT-3';
mouse *Sirt1*, forward primer 5'-TGAGCTGGATGATATGACGC-3' and reverse primer 5'-GGAAGTCCACCGCAAGG -3';
mouse *Ppargc1a*, forward primer 5'-TATGGAGTGACATAGAGTGTGCT-3' and reverse primer 5'- CCACTTCAATCCACCCAGAAAG-3';
mouse *cyclophilin*, forward primer 5'-ATGGCAAATGCTGGACCAAA-3' and reverse primer 5'-CATGCCTTCTTTCACCTTCCC-3';

Heat stress resistance assays

Heat stress assays in *C. elegans* were performed as described previously (3) with minor modifications. About 100 adult worms (day 4) per group were transferred to 3 new RNAi NGM plates with RNAi bacteria. The number of dead worms on each plate was scored every 2 hours for the first 8 hours after shifting to 35^{o}C. Survival was determined as described for lifespan analysis.

Supplemental References

1. Baur JA, *et al.* (2006) Resveratrol improves health and survival of mice on a high-calorie diet. *Nature* 444(7117):337-342.
2. Ernst J & Bar-Joseph Z (2006) STEM: a tool for the analysis of short time series gene expression data. *BMC Bioinformatics* 7:191.
3. Chen D, Thomas EL, & Kapahi P (2009) HIF-1 modulates dietary restriction-mediated lifespan extension via IRE-1 in Caenorhabditis elegans. *PLoS Genet* 5(5):e1000486.

Supplemental Figures

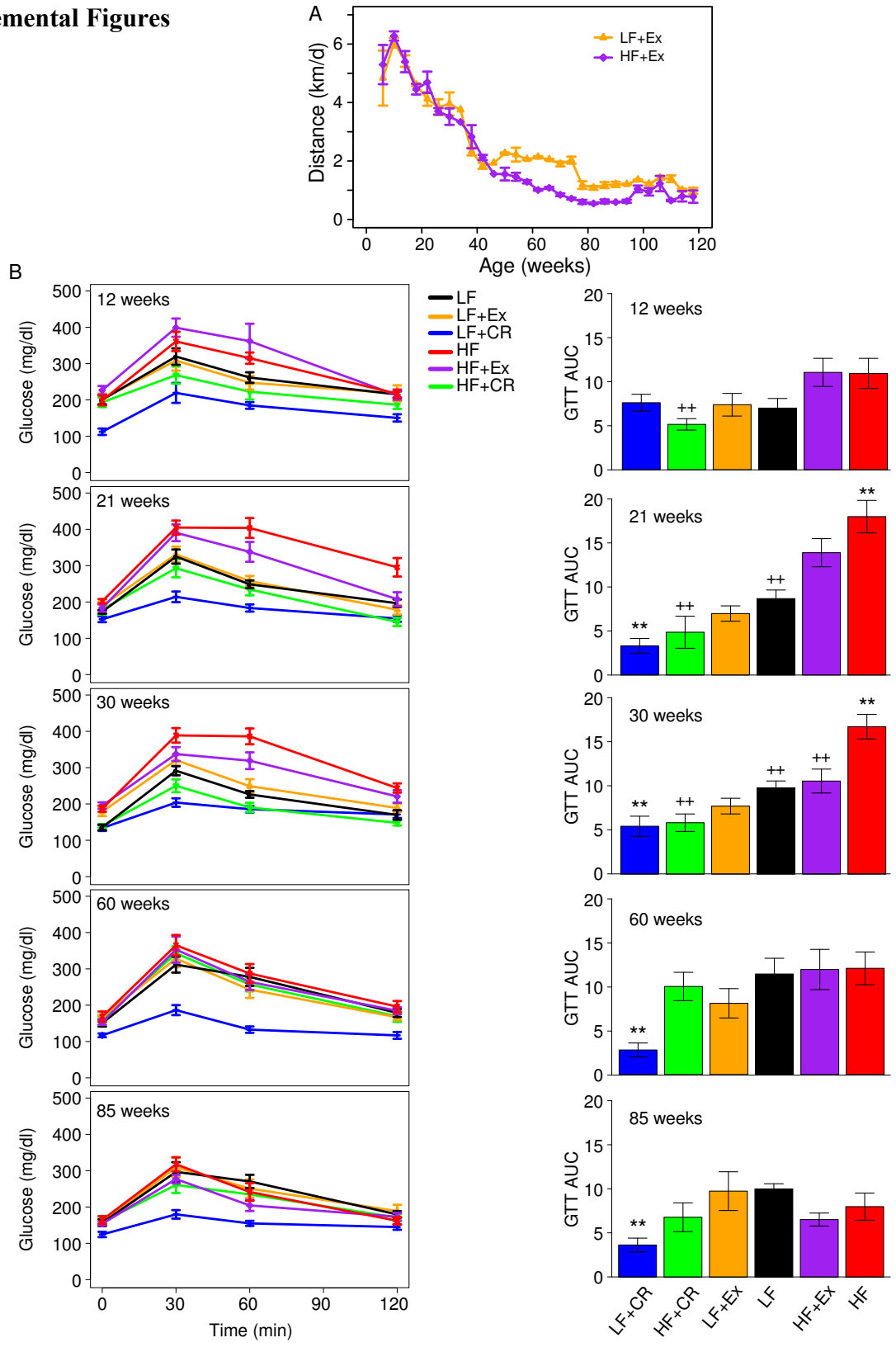

Figure S1. Exercise monitoring and glucose tolerance of mice. (**A**) Voluntary running distance was recorded and the average running distance was plotted biweekly for mice fed LF or HF in the exercise groups (n>6). (**B**) Glucose tolerance test (GTT) was performed at the indicated ages for each intervention group (n=8-10 per group). In the left panels, the blood glucose levels are plotted against the times after i.p. injection of 1 g/kg glucose. Shown in the right panels are the calculated areas under the curve (AUC) of blood glucose, presented as mean ± SEM, $^{**}P < 0.01$ versus LF, and $^{++}P < 0.01$ versus HF tested by ANOVAs.

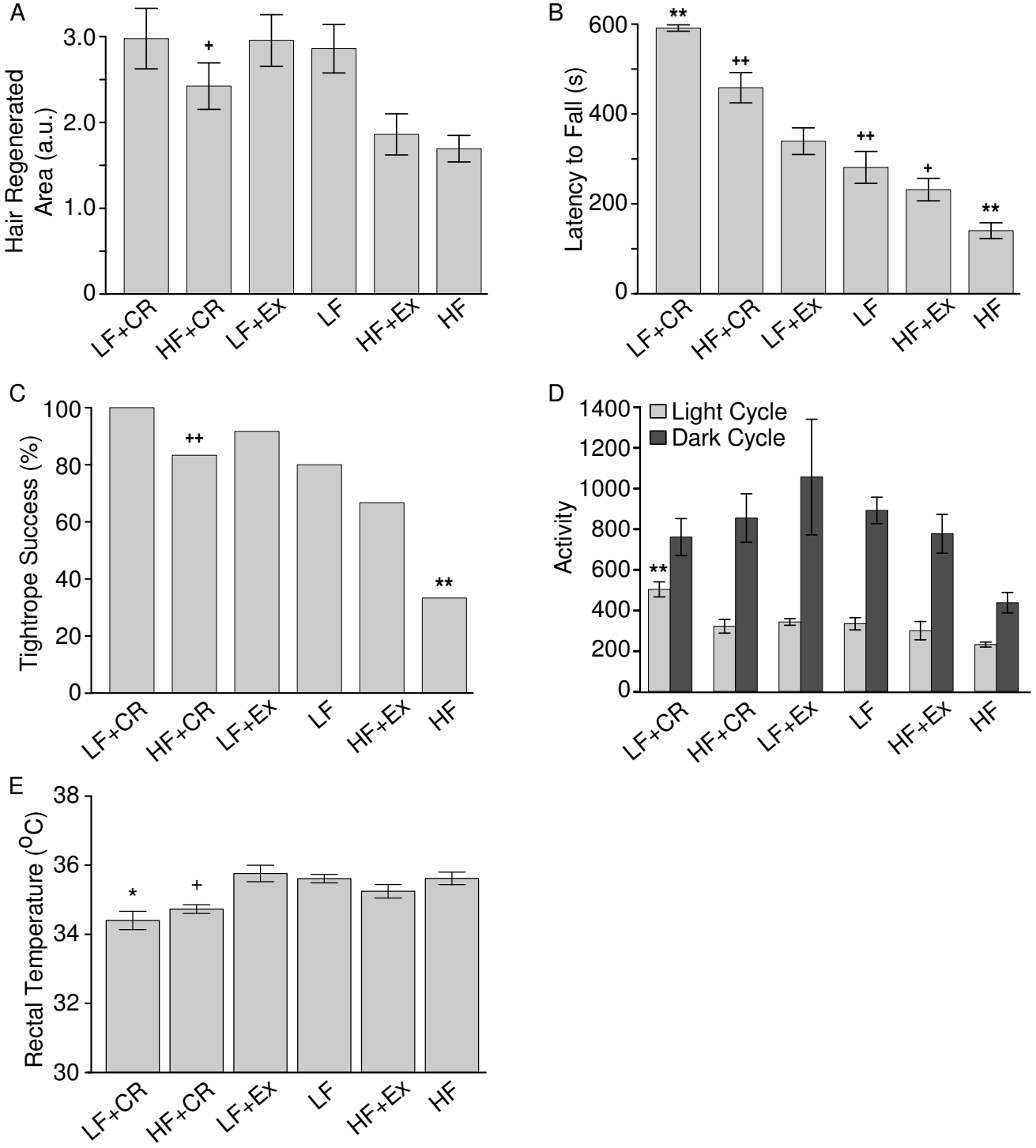

Figure S2. Aging-sensitive markers, midlife physical activity and body temperature of mice. (**A-C**) Aging-sensitive markers. (**A**) Hair re-growth assay for mice at 90 weeks of age (n=9-12 per group). Hair re-growth capacity of the dorsal skin was scored at 21 days after shaving and quantified in arbitrary units (a.u.). (**B**) Rotarod tests for mice at 85 weeks of age. Shown are the maximal time to fall from the accelerating rotarod, averaged from three trials per mouse (n=11-12 per group). (**C**) Tightrope test for mice at 85 weeks of age. The percentage of mice passing the test is shown for each group (n=8-12 per group). (**D**) Physical activity during the light and dark cycles was determined by CLAMS for mice at 57-58 weeks of age (n=5 per group). (**E**) Rectal temperatures of mice at 90 weeks of age (n=10 per group). Data are presented as mean ± SEM, $^{*}P < 0.05$, $^{**}P < 0.01$ versus LF, and $^{+}P < 0.05$, $^{++}P < 0.01$ versus HF tested by ANOVAs.

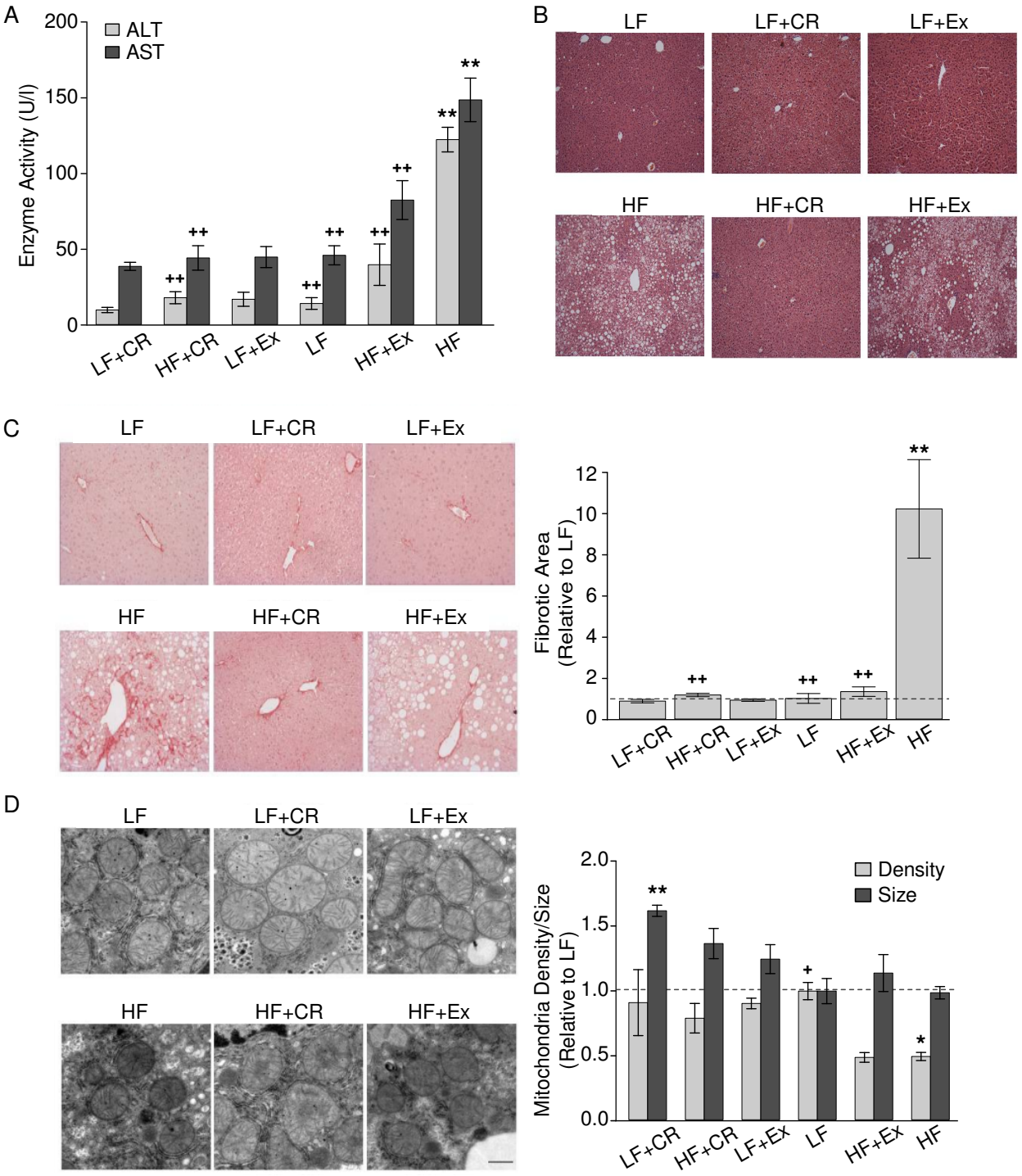

Figure S3. Liver functions affected by the diet interventions. Liver functions were measured in mice (n=8 per group) that were sacrificed at 62 weeks of age. (**A**) Liver function was assessed by the serum abundance of alanine aminotransferase (ALT) and aspartate aminotransferase (AST). (**B**) Representative images of liver sections of mice of each indicated group (n=4-5 per group) that were subjected to hematoxylin and eosin staining. Original magnification: 20X. (**C**) Evaluation of liver fibrosis by Sirius-Red staining for collagens. Representative images are shown. Original magnification, 20X. The extent of fibrosis was quantified as the percentage of Sirius-Red positive area (n=4 per group). (**D**) Mitochondrial density and size. Liver sections were analyzed by transmission electron microscopy. Shown are representative images at a magnification of 6,000. Mitochondrial densities were determined by normalizing the counted number of mitochondria to the area of each randomly selected cell (n=30 cells for each group). Quantification of mitochondrial size was performed for 4 mice from each group. Data are shown as mean ± SEM, $^{*}P < 0.05$, $^{**}P < 0.01$ versus LF, and $^{+}P < 0.05$, $^{++}P < 0.01$ versus HF by ANOVAs.

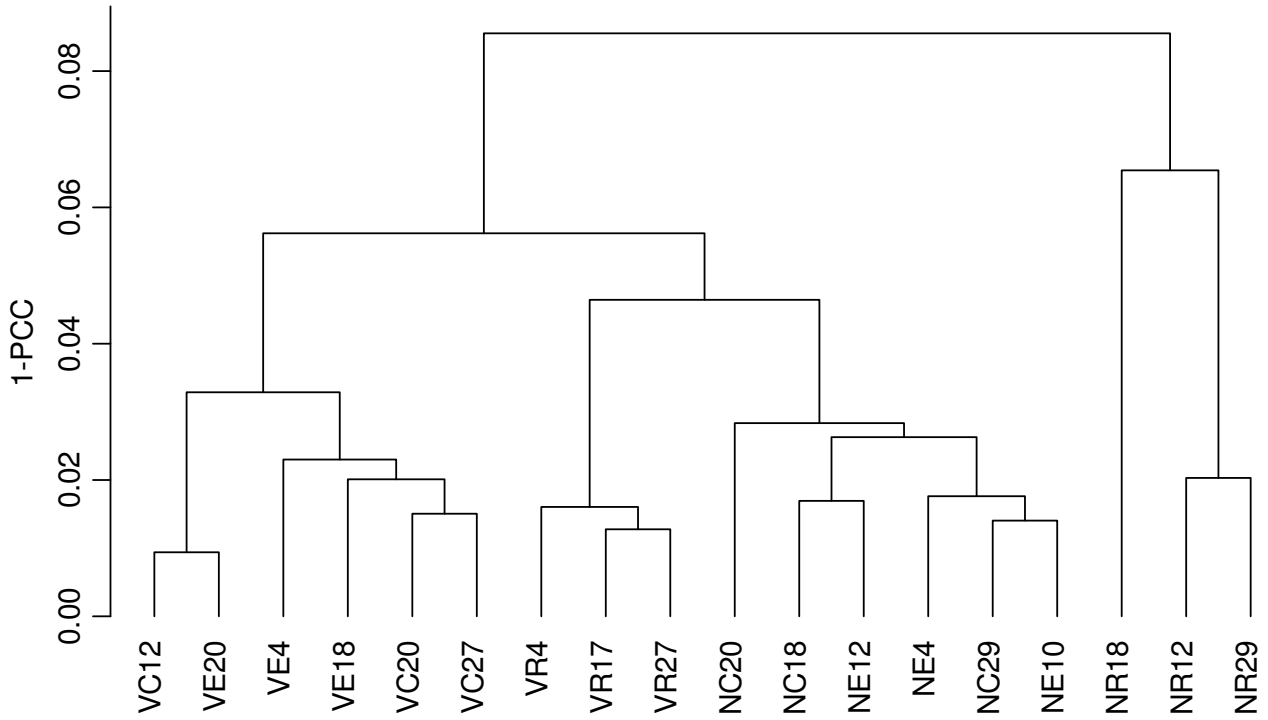

Figure S4. Hierarchical clustering of the samples based on the differentially expressed genes (Methods). The sample prefix 'VC' represents HF group, 'VE' HF+Ex, 'VR' HF+CR, 'NC' LF, 'NE' LF+Ex and 'NR' LF+CR, respectively.

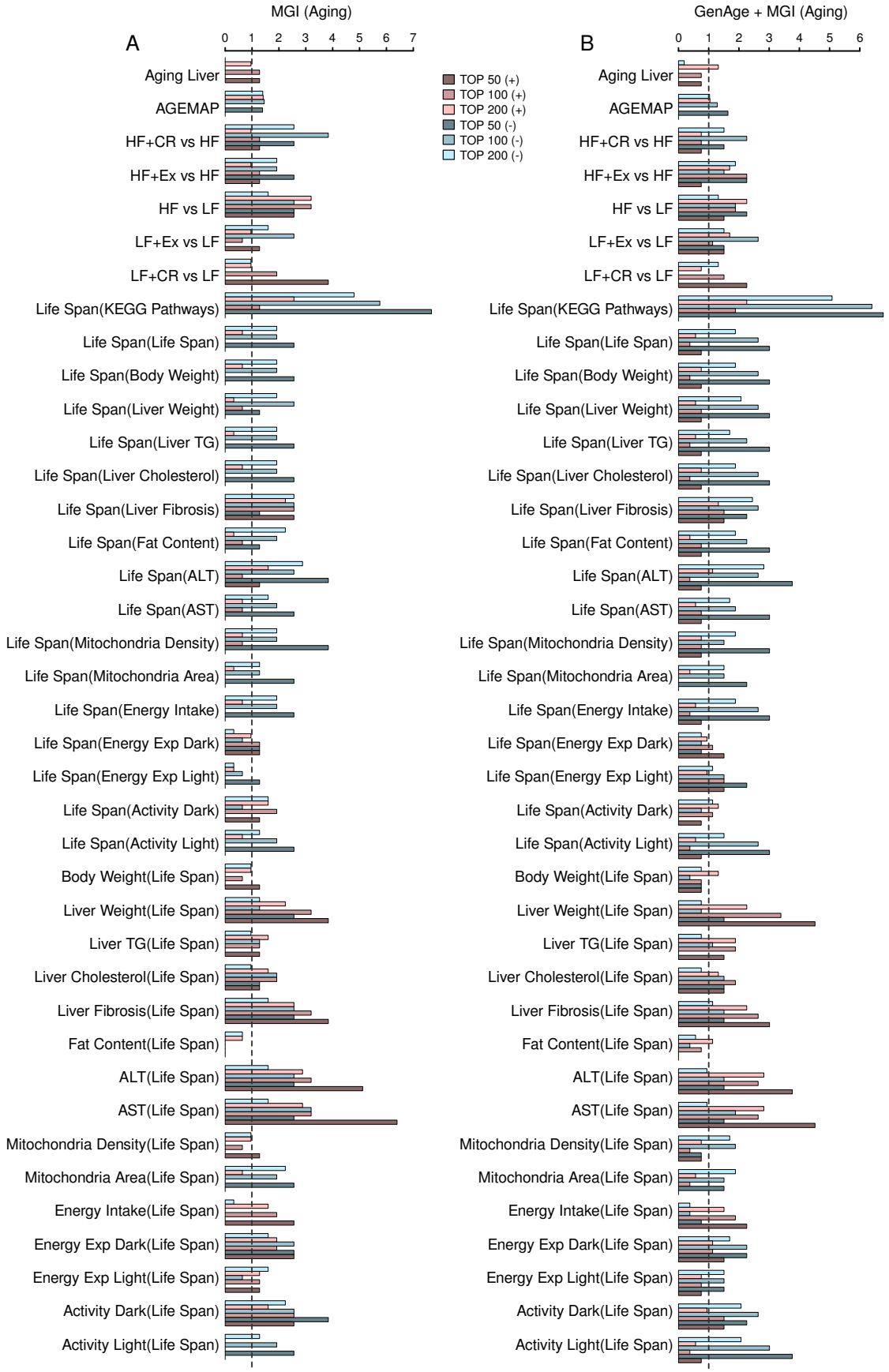

Figure S5. Fold of enrichments over the background of lifespan correlated or anti-correlated genes, significantly differentially expressed genes between any single pair of treatments, lifespan/aging related genes in AGEMAP, and our aging liver time-course dataset on (**A**) MGI aging dataset and (**B**) combination datasets of GenAge, MGI aging and reviews recruited manually.

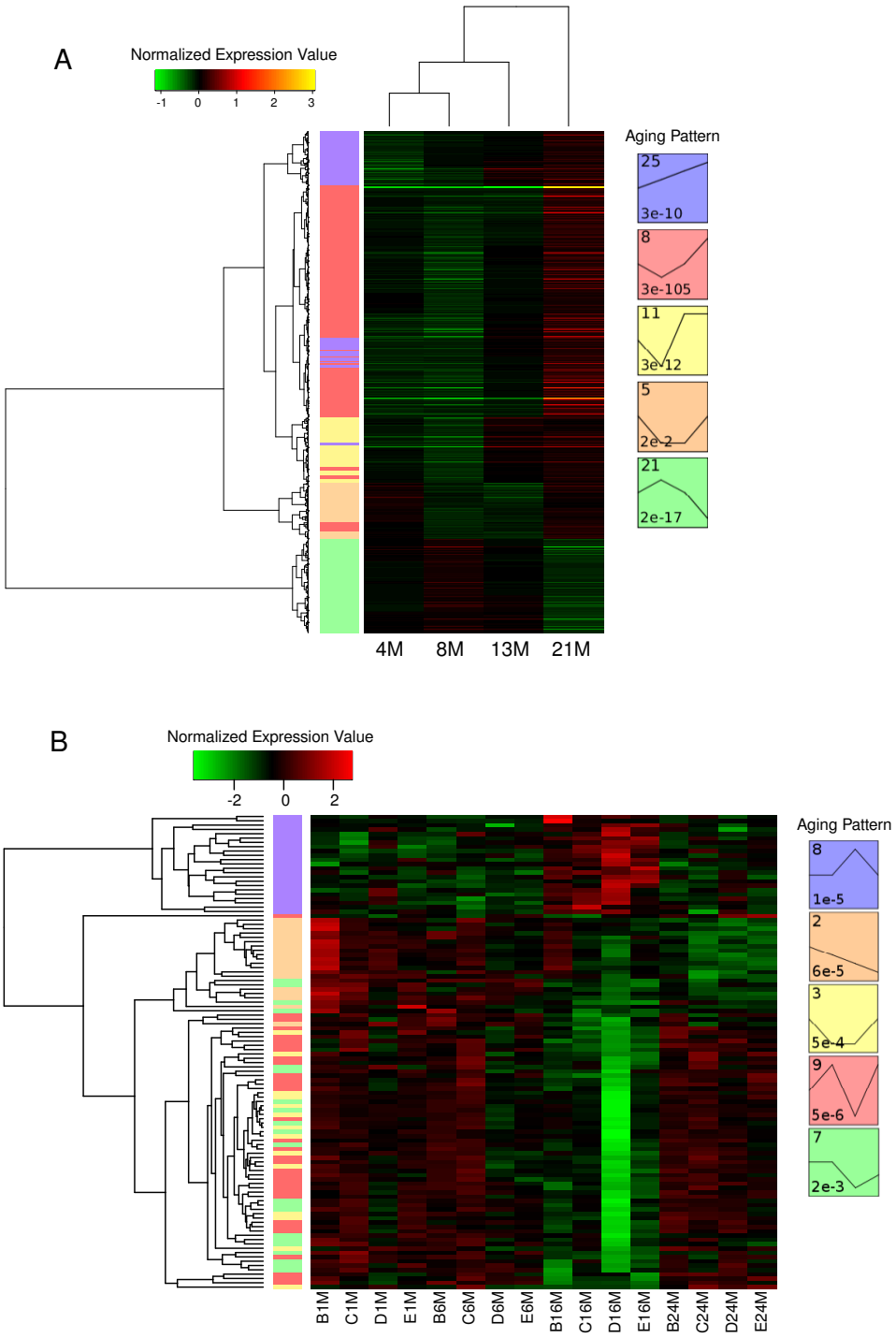

Figure S6. Hierarchical clustering of the expression profiles of age-related genes based on microarray profiles from mice at 4, 8, 13 and 21 months of age (**A**), or based on AGEMAP liver expression profiles (**B**) constituting the significant age-dependent gene expression patterns determined by STEM ($P < 0.01$).

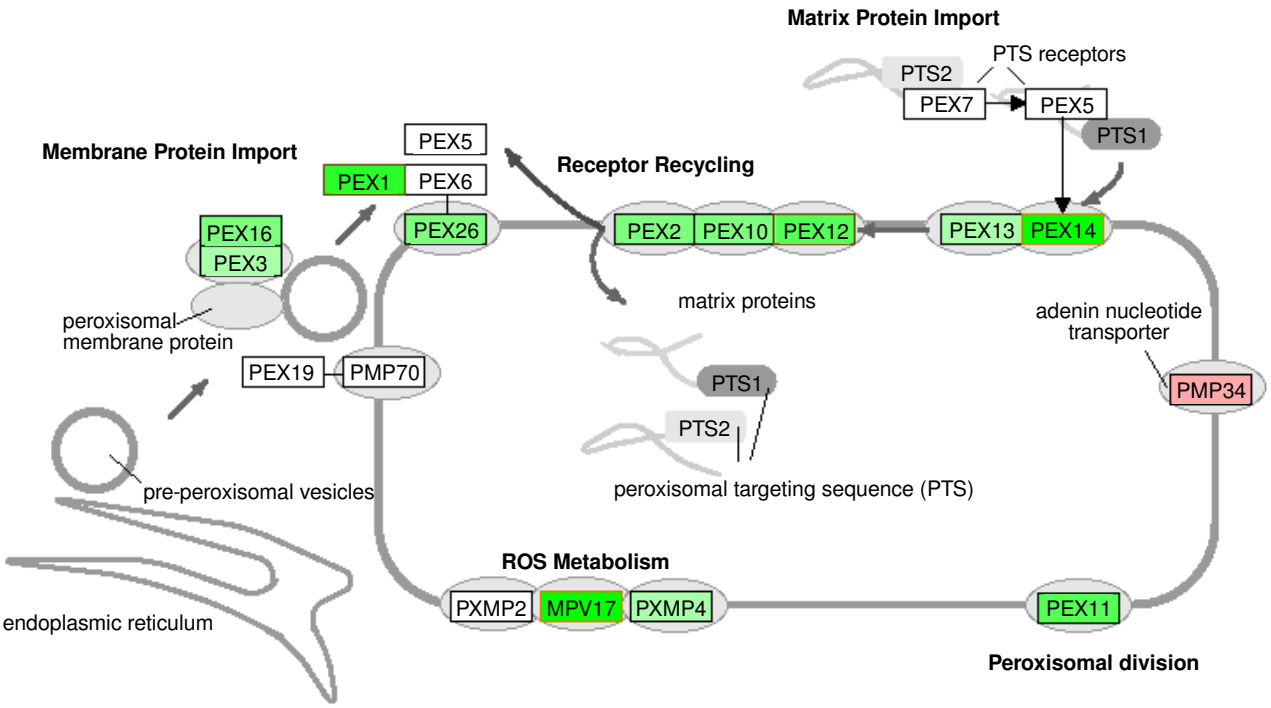

Figure S7. KEGG 'peroxisome' pathway with each gene (node) color-coded for its correlation to the mean lifespan across the six dietary groups according to the color key. Red color represents positive correlation between PEX genes and lifespan, while green color indicates negative correlation.

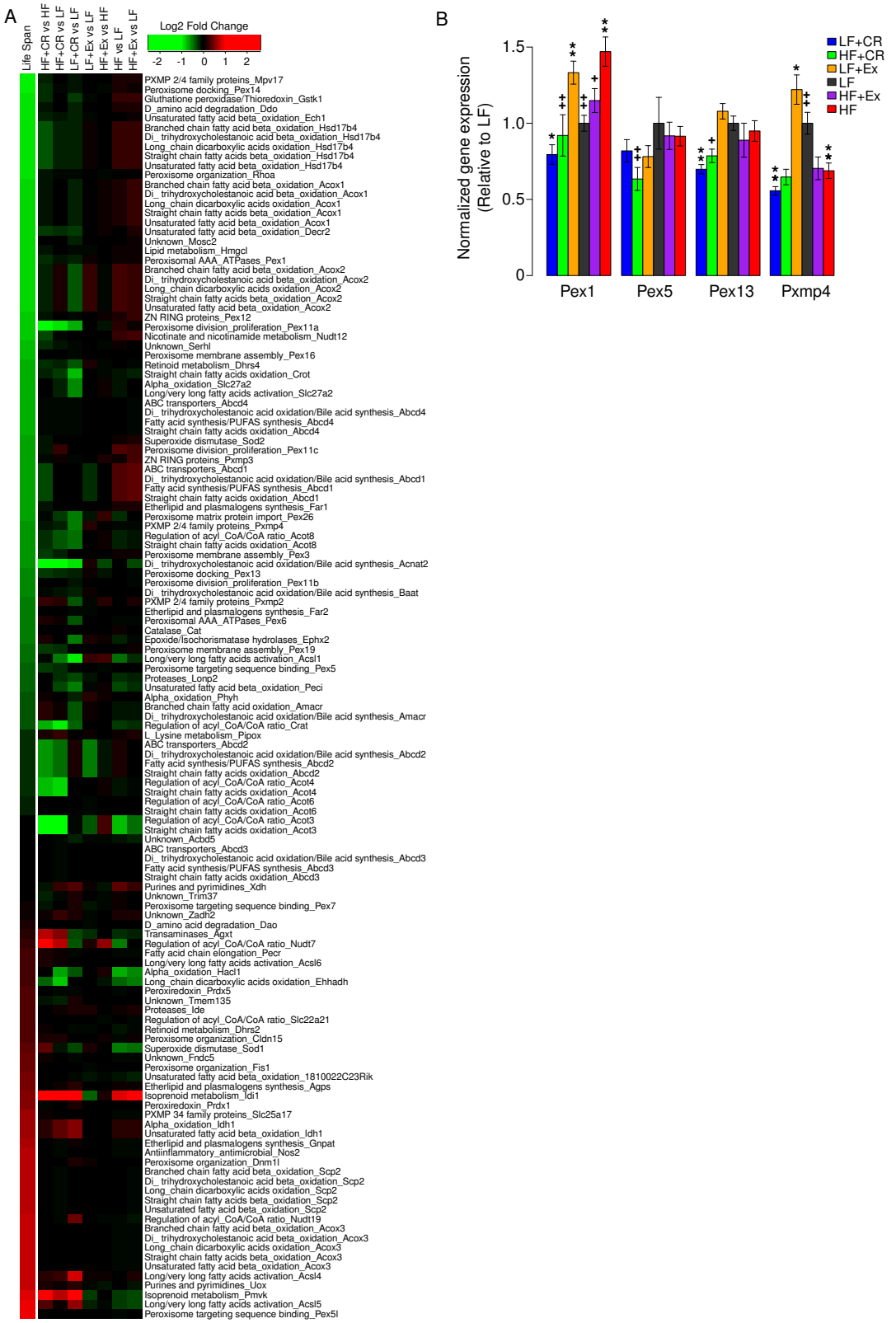

Figure S8. Gene-wise analysis of peroxisomal function categories. (**A**) With each peroxisomal function category, the correlation (PCC) of each gene's expression level with lifespan across the six different treatment groups and the fold changes between seven comparisons as indicated are visualized in the heatmap according to the color keys. (**B**) The midlife expression levels of the indicated four hepatic PEX genes, which showed negative correlation with the lifespan of mice through microarray analysis, were confirmed by real-time quantitative PCR. Data are presented as mean ± SEM (n=8/group). $^{*}P$ <0.05, $^{**}P$<0.01 versus LF, and $^{+}P < 0.05$, $^{++}P < 0.01$ versus HF by ANOVAs.

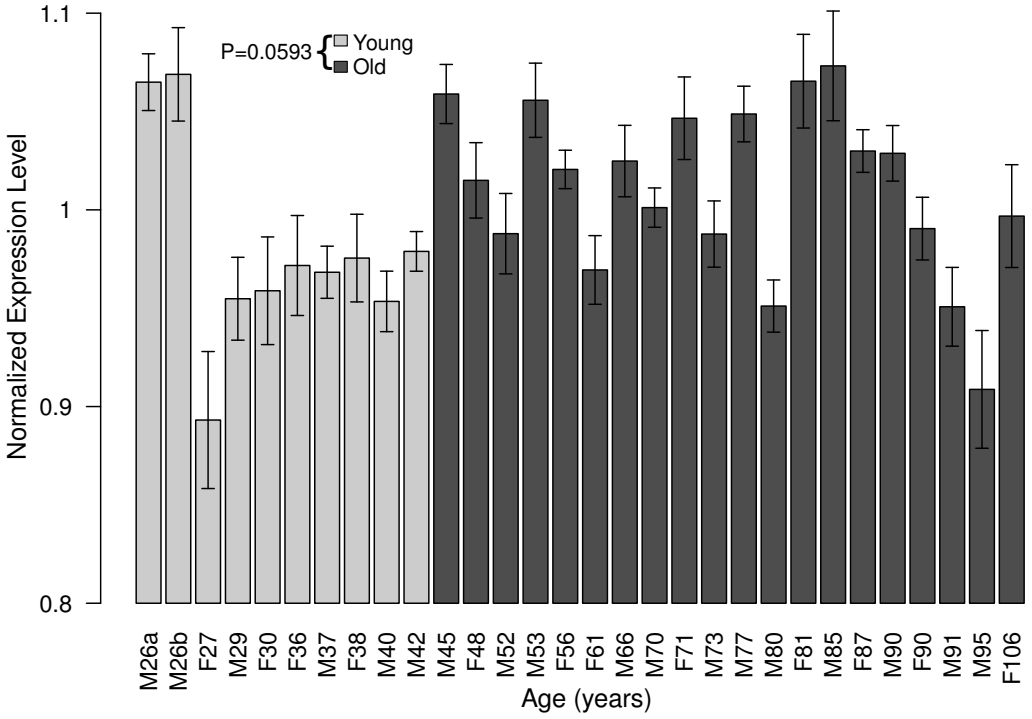

Figure S9. Expression level changes of the proxisomal proliferation genes (PEX) during human brain aging. Average and standard deviation of the log2 expression levels of the 11 PEX genes in each of the 30 sample are shown by the height of the bar and whisker, respectively.

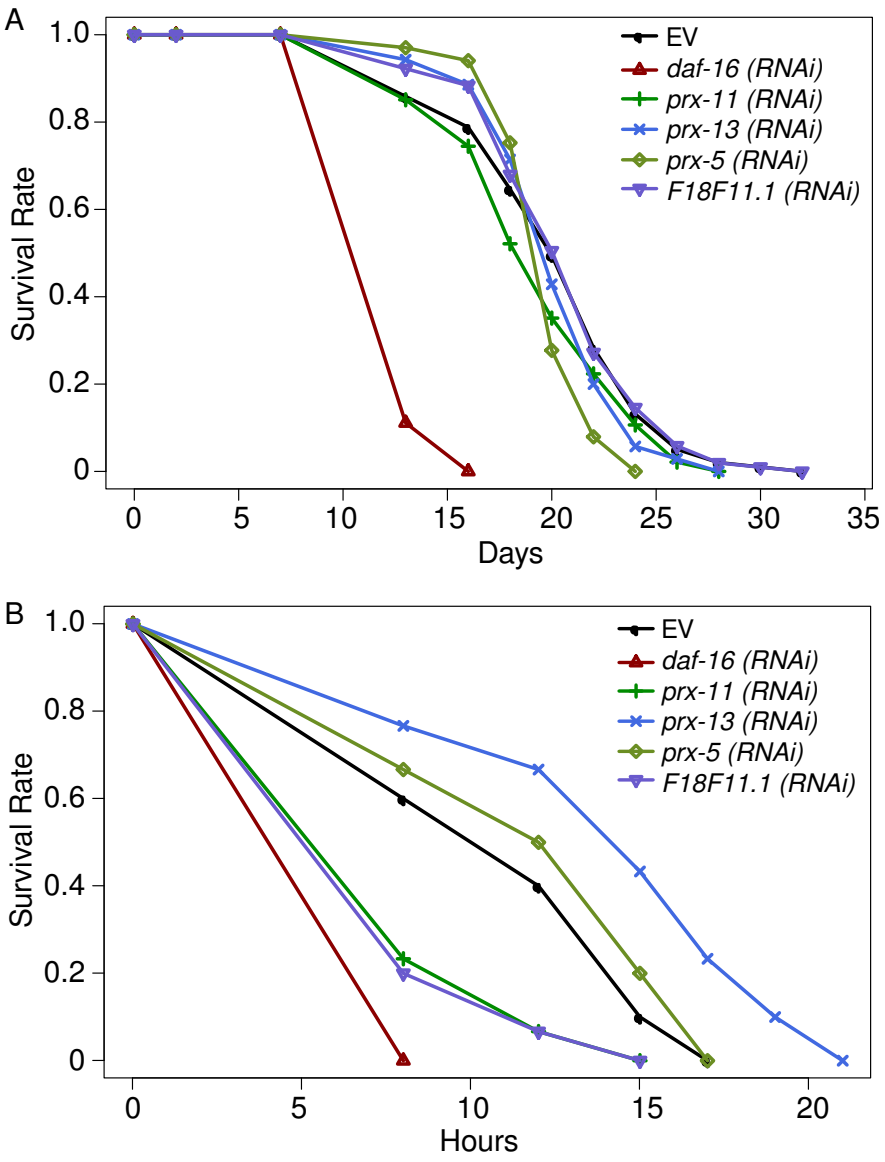

Figure S10. Survival curves of the N2 stain of worms with RNAi knockdown of *prx* genes starting from L1 **(A)** or in response to heat stress at 35°C **(B)**.

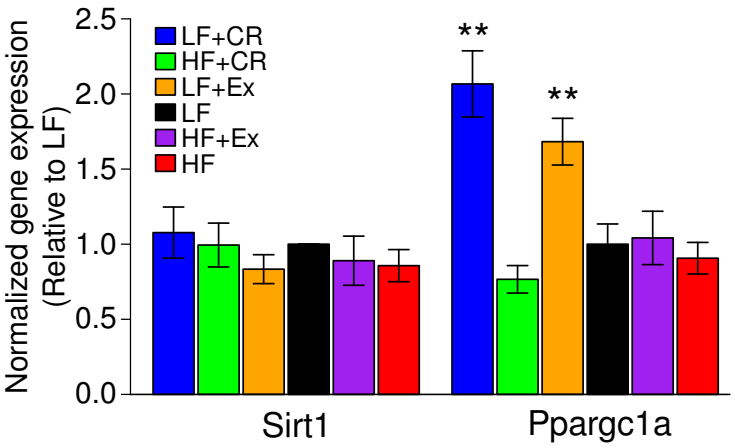

Figure S11. Hepatic expression levels of *Sirt1* and *Ppargc1a* in the six intervention groups of mice. Real-time quantitative RT-PCR was performed, and data are presented as mean ± SEM (n=8/group). ***P*<0.01 versus LF by ANOVAs.

Supplemental Tables

Table S1. Metabolic biomarkers in mice of the six intervention groups at 60~62 weeks of age.

	Parameter	LF+CR	HF+CR	LF+Ex	LF	HF+Ex	HF
Serum	Triglycerides (mg/dl)	14.53 (3.63)	13.23 (5.07)	14.88 (2.84)	18.85 (5.58)	24.48 (5.64)	27.425 (2.16)
	Cholesterol (mg/dl)	64.18 (7.72)$^{\#\#**}$	140.37 (17.40)$^{\#\#}$	106.32 (6.82)$^{\#\#}$	121.73 (8.18)$^{\#\#}$	200.17 (14.64)$^{\#}$	243.97 (17.10)**
	insulin (ng/ml)	0.48 (0.03)$^{\#\#}$	0.89 (0.16)$^{\#\#}$	0.65 (0.06)$^{\#\#}$	0.52 (0.08)$^{\#\#}$	3.80 (0.77)	3.46 (0.56)**
	leptin (ng/ml)	0.83 (0.14)$^{\#\#**}$	10.04 (1.04)$^{\#\#}$	2.12 (0.09)$^{\#\#}$	5.14 (0.38)$^{\#\#}$	53.6 (12.17)	72.09 (5.53)**
	GTT AUC	2.79 (0.79)**	9.99 (1.61)	8.09 (1.67)	11.41 (1.79)	11.93 (2.28)	12.06 (1.85)
Liver	Liver weight (g)	1.21 (0.04)$^{\#\#}$	1.26 (0.05)$^{\#\#}$	1.26 (0.06)$^{\#\#}$	1.37 (0.05)$^{\#\#}$	2.43 (0.26)	2.98 (0.17)**
	Triglycerides (mg/dl)	14.79 (1.90)$^{\#\#**}$	27.50 (2.16)$^{\#\#}$	29.30 (3.84)$^{\#\#}$	30.80 (3.19)$^{\#\#}$	65.84 (7.08)	71.36 (5.43)**
	Cholesterol (mg/dl)	2.18 (0.23)	2.26 (0.26)	2.77 (0.31)	3.15 (0.31)	3.40 (0.35)	3.53 (0.32)

Values shown are mean (± SEM).

**P<0.01 versus LF, $^{\#}$ P<0.05 and $^{\#\#}$ P<0.01 versus HF by two-way ANOVA.